

Title: Selective generation of reactive oxygen species in plasma activated water using CO₂ plasma

Authors

Vikas Rathore^{1,2*} and Sudhir Kumar Nema^{1,2}

1. Atmospheric Plasma Division, Institute for Plasma Research (IPR), Gandhinagar, Gujarat 382428, India

2. Homi Bhabha National Institute, Training School Complex, Anushaktinagar, Mumbai 400094, India

***Email: vikas.rathore@ipr.res.in**

Abstract

In the present work, a process of a selective generation of reactive oxygen species (ROS) such as H₂O₂ and dissolved O₃ in plasma-activated water (PAW) is discussed. For selective ROS generation, pure CO₂ was used as a plasma-forming gas. The gases species present in plasma and properties of PAW are compared in details when CO₂ and air are used as plasma forming gas. The results reveal that PAW (CO₂) has significantly higher pH, and low oxidizing potential and electrical conductivity compared to PAW (air). The formed species in PAW (CO₂) due to CO₂ plasma-water interaction are dissolved O₃, H₂O₂, dissolved CO₂, and CO₃²⁻ ions, etc. In addition, no detectable concentration of NO₂⁻ and NO₃⁻ ions is observed in PAW (CO₂). PAW (CO₂) has a substantially higher concentration of H₂O₂ compared to PAW (air). Moreover, increasing plasma treatment time with water significantly increases H₂O₂ and dissolved O₃ concentration in PAW (CO₂). However, PAW (air) showed a rise and fall in H₂O₂ and dissolved

O₃ concentration with time. In conclusion, selective generation of ROS in PAW is possible using CO₂ as plasma-forming gas.

Keywords: Plasma activated water, CO₂ plasma, CO₂ emission spectra, reactive oxygen-nitrogen species,

Introduction

The plasma-activated water (PAW) technology is one of the fastest growing novel technologies in cold plasma field. This is due to its continuously evolving applications in the field of plasma medicine, plasma agriculture, plasma food science and technology, etc. (1-11). These applications of PAW are possible due to the presence of various stable reactive oxygen-nitrogen species (RONS) in it. These RONS in PAW are formed as a resultant product of plasma-water interaction. Moreover, it brings a physicochemical change in PAW properties such as pH, oxidizing potential, and electrical conductivity, etc. (4, 9-16)

Different RONS have different significance in their applications (2, 4, 5, 17). Such as species like H₂O₂, dissolved O₃, HO·, and ONOO⁻ have applications in microbial inactivation, selective killing of cancer cells, enhancing the shelf life of various food products such as fruits, vegetables, meat, seafood, and dairy products, etc. (1, 3-5, 8-11, 17, 18) Moreover, reactive nitrogen species can be used as a nitrogen replacement source for numerous agriculture applications (2, 7, 15, 19-21).

The PAW produced due to plasma-water exposure contains both the reactive oxygen species (H₂O₂, dissolved O₃, HO·, etc.) and reactive nitrogen species (NO₂⁻ ions, NO₃⁻ ions, etc.) (4, 13, 22). This is due to conventionally used plasma forming gases during PAW production which contain oxygen and nitrogen molecules or ionization of surrounding air by noble gas. The frequently used plasma-forming gases at atmospheric pressure during PAW production are air, nitrogen (N₂), oxygen (O₂), argon (Ar), Helium (He), and their mixture in

different compositions (4, 7, 9, 11, 13, 18, 23). Working with 100% O₂ plasma at atmospheric pressure is not recommended. Since, O₂ is highly oxidizing and can ignite flammable material rapidly that can cause explosions at atmospheric pressure. The use of inert gases (Ar or He) for plasma production mainly discharges the atmospheric air resulting in the generation of various RONS during plasma-water exposure (23). Hence, the production of plasma-activated water with a selective generation of ROS (free from nitrogen species) at atmospheric pressure is still an open challenge to be overcome. The presence of RNS forms nitrous and nitric acid (strong acid) in PAW due to which the pH of PAW decreased substantially. Therefore, PAW cannot be used in applications that do not prefer low pH solutions. Due to this applicability of PAW is restricted and also one of the main disadvantages of PAW. As per the authors' knowledge, no work has been reported that emphasizes the selective generation of reactive oxygen species (ROS). The ROS have applications in microbial and biofilm inactivation, medicine, food preservation, and enhancing seeds germination, etc (2-4, 8, 9, 24). This research gap tries to be fulfilled in present work.

The conventionally used oxidizing and inert gases plasma formed nitrogen species in water as discussed above (4, 7, 9, 11, 13, 18, 23). Moreover, nitrogen free gases such as phosphine (PH₃), hydrogen sulphide (H₂S), arsine (AsH₃) and sulphur dioxide (SO₂), etc. have environmental hazards (highly toxic) at atmospheric pressure, hence not recommended. Therefore, the present work uses CO₂ as plasma forming gas for selective generation of reactive oxygen species in plasma-activated water. Moreover, the PAW produced using CO₂ plasma is also compared with PAW produced using air plasma. The comparison was performed based on plasma characterization, formation of plasma reactive species/radicals, and properties of PAW.

Material and Methods

Experimental Setup

The experimental schematic of characterization of air and CO₂ plasma and production of plasma-activated water (PAW) is shown in figure 1. The air and CO₂ plasma were produced in a co-axial cylindrical pencil plasma jet (PPJ)(25). The PPJ setup based on the principle of dielectric barrier discharge and the schematic is shown in figure 1. In which the central ground electrode was made using a 1.6 mm tungsten rod. The high voltage electrode was made from copper in cylindrical form with an inner diameter of 6 mm in which dielectric quartz tube (outer diameter × inner diameter – 6 mm × 4 mm) was tightly fixed. The discharge gap between the dielectric surface and the ground electrode was 1.2 mm.

To measure the voltage drop across the PPJ setup a 1000x voltage probe (Tektronix P6015A) and a 100 MHz bandwidth, 2 Gs s⁻¹ sampling rate, and a 4-CH oscilloscope (Tektronix TDS2014C) was used (26). A 10x (Tektronix TPP0201) voltage probe was used to measure the current and transported charge. This probe measured the voltage drop across the resistor (R - 30 Ω) and capacitor (C - 100 μF) connected in series with the ground as shown in figure 1. The air and CO₂ plasma emission spectra were measured by capturing the afterglow light photons using optical fiber and a spectrometer (Plasma and Vacuum Solution (PVS), model UVH-1) as shown in figure 1.

For plasma-activated water production, 50 ml of ultrapure milli-Q water was taken in 600 ml of a glass beaker. This water was treated with air and CO₂ plasma as shown in figure 1. The air and CO₂ gas flow rate were controlled using a flow controller and the flow rate was fixed at 3 l min⁻¹. To enhance the solubility of plasma produced reactive species in water and escalate the reaction between gases reactive species and water, a continuous stirring of water and cooling of water were performed. For water stirring, a mortarless magnetic stirrer was used and for cooling of water, ice-cooled water was placed in contact with a glass beaker in which PAW was kept during plasma-water interaction.

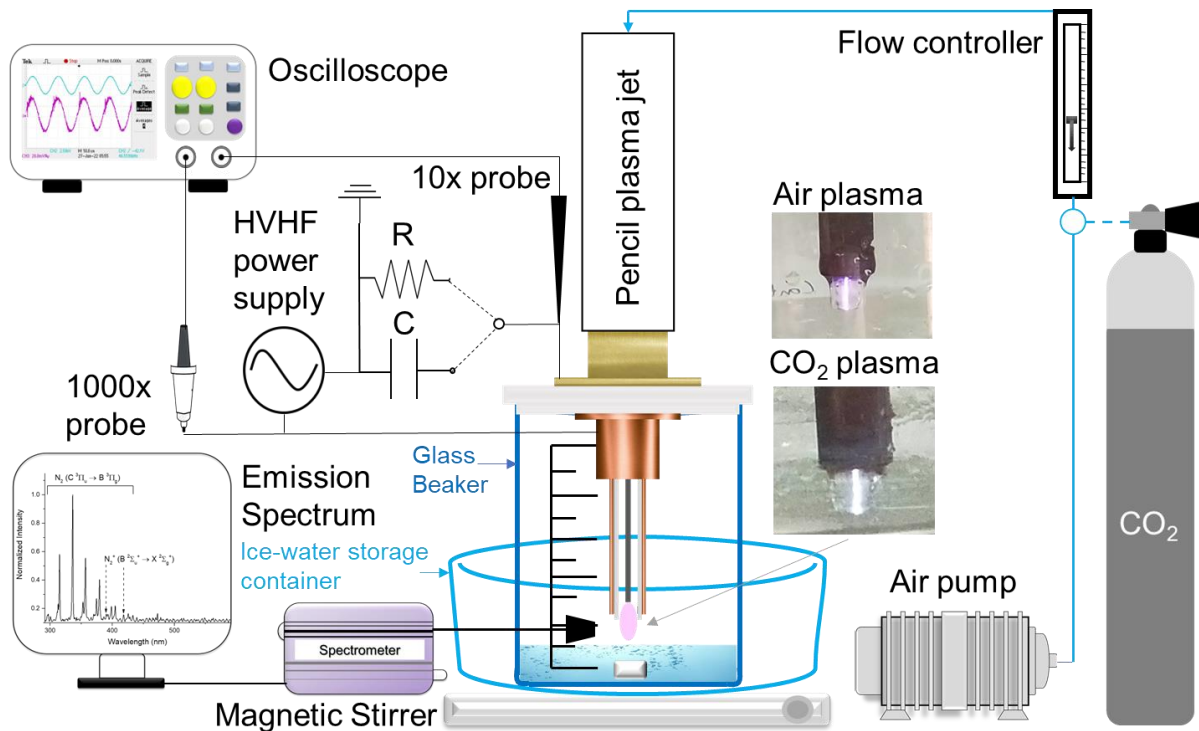


Figure 1. Schematic of production of plasma activated water using CO₂ and air plasma and these gases plasma electrical and optical emission characterization.

Equipments used for measurement of physicochemical properties of PAW

The physicochemical properties of PAW (air or CO₂) such as pH, oxidation-reduction potential (ORP), total dissolved solids (TDS), and electrical conductivity (EC) were measured for PAW characterization. A Hanna Instruments pH meter (HI98121), HM digital ORP meter (ORP-200), HM digital TDS meter (AP-1), and Contech Instruments Ltd. EC meter (CC-01) were used to measure the pH, ORP, TDS, and EC of PAW.

Measurement of Reactive Oxygen-Nitrogen Species Concentration

The reactive oxygen-nitrogen species (RONS) form in PAW (air or CO₂) due to air plasma or CO₂ plasma water interaction was determined semi-quantitatively and quantitatively. Strip test and colorimetry test kits were used to determine the initial RONS concentration in PAW and plasma (VISOCOLOR alpha (MACHEREY-NAGEL item no. 935065) nitrate (NO₃⁻) ions

colorimetry test kit, dissolved O₃ test kit (Hanna Instruments item no. HI38054), H₂O₂ determination test strips (QUANTOFIX Peroxide 25, MACHEREY-NAGEL item no. 91319), NO₂⁻ ions determination test strips (QUANTOFIX Nitrite, MACHEREY-NAGEL item no. 91311), gases O₃ determination test strips (Ozone Test for Ozone in air, MACHEREY-NAGEL item no. 90736)).

The quantitative estimation of RONS concentration present in PAW was measured spectrophotometrically. The NO₃⁻ ions concentration was measured using the ultraviolet screening method (27), and the standard curve of NO₃⁻ ions was made using NaNO₃ solution with molar attenuation coefficient 0.0602 (mg L⁻¹)⁻¹(25). In acidic region, NO₂⁻ ions present in the solution when react with the reaction mixture of N-(1-naphthyl) ethylenediamine dihydrochloride and sulfanilamide give reddish purple azo dye ($\lambda_{\max} = 540 \text{ nm}$)(27). This characteristic of NO₂⁻ ions was utilized to determine its unknown concentration. The standard curve of NO₂⁻ ions was made using NaNO₂ solution with a molar attenuation coefficient of 0.0009 ($\mu\text{g L}^{-1}$)⁻¹(25). The unknown concentration of H₂O₂ in PAW was determined spectrophotometrically using the titanium sulfate method (13). The standard curve of H₂O₂ was made of 30% H₂O₂ solution (molar attenuation coefficient 0.4857 mM⁻¹(25)). The unknown concentration of dissolved O₃ in PAW was determined using the indigo colorimetric method (27).

The titratable acidity and dissolved CO₂ concentration in PAW (CO₂) were determined using the titration method(8, 28). The titratable acidity of PAW (CO₂) was determined using 0.1 M sodium hydroxide (NaOH) solution and a freshly prepared phenolphthalein indicator. In addition, the dissolved CO₂ concentration in PAW was determined using 0.02 N sodium carbonate (Na₂CO₃) solution and freshly prepared phenolphthalein as an indicator (28). The dissolved carbonate ions (CO₃²⁻) concentration in PAW (CO₂) was determined using the UV screening method (29, 30) with CO₃²⁻ molar attenuation coefficient 0.0008 (mg L⁻¹)⁻¹.

Data analysis

All the experimental were performed at least three times ($n \geq 3$) in the present investigation. The results were shown as $\mu \pm \sigma$ (mean \pm standard deviation (Error)). The statistically significant difference with a significant level of 95% ($p = 0.05$) among the groups mean were calculated using one-way analysis of variance followed by a post-hoc test (Fischer Least Significant Difference (LSD)).

Results and discussion

Voltage current waveform

The air and CO₂ plasma voltage current waveform produced in dielectric barrier discharge (DBD) pencil plasma jet (PPJ) is shown in figure 2. The air and CO₂ plasma current waveform showed nanosecond (ns) current filaments peaks (~ 100 ns, shown in figure S1 of supplementary material) over each negative and positive current half cycle. The cluster of these nanosecond current filaments lies in the microsecond region. Therefore, these current discharges are known as filamentary DBD micro discharges (26). The discharge current peaks observed in CO₂ plasma were higher than air plasma for the same applied voltage. This signifies the radicals and species produced in CO₂ plasma had higher current carrying affinity compared to air plasma. Alongside, the other possible region is the generation of high concentration of plasma radicals and species in CO₂ plasma compared to air plasma. Due to which high discharge current was observed in CO₂ plasma for the same process parameter.

The plasma discharge power consumed during the air and CO₂ plasma generation was measured using voltage-transported charge Lissajous figure. Initially, the energy consumed during discharge was calculated using the integral of voltage over the charge domain. For power calculation, a product of energy consumed with frequency (40 kHz) was performed. To

compare the properties of PAW produced using air and CO₂ plasma, the energy and power kept in the range of 0.0125 mJ to 0.015 mJ and 0.5 to 0.6 W.

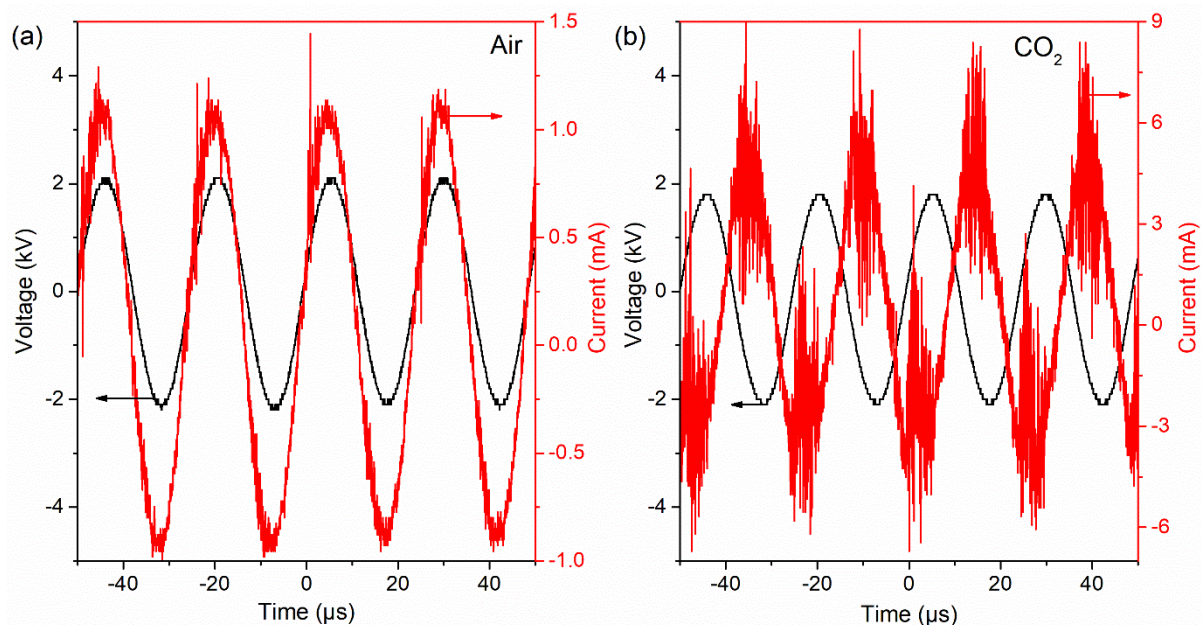


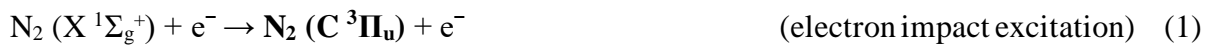
Figure 2. Voltage current waveform of (a) air and (b) CO₂ plasma produced in pencil plasma jet

Optical emission spectra of air and CO₂ plasma

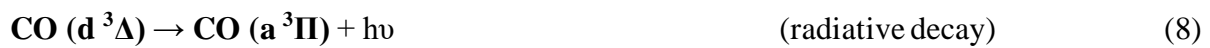
The optical emission spectra of air and CO₂ plasma in the afterglow region are shown in figure 3. The overlay plot of air (solid line) and CO₂ (dotted lines) plasma showed the deviation between the emission bands peaks lines of air and CO₂ plasma. These emission bands peaks lines are formed due to electronic transition radiative decay of the upper vibration state to the lower vibration state of ions or molecules. The emission spectrum of air plasma consists of strong emission band peaks of N₂ second positive system ($C^3\Pi_u \rightarrow B^3\Pi_g$) along with weak emission intensity band peaks of N₂⁺ first negative system ($B^2\Sigma_u^+ \rightarrow X^2\Sigma_g^+$) (31, 32). The reactions associated with this transition are shown in equations (1-4). Moreover, the CO₂ plasma afterglow region showed strong intensity emission band peaks of CO₂⁺ first negative system ($A^2\Pi_g \rightarrow X^2\Pi_u$). Along with that weak intensity emission band peaks of CO⁺ ($A^2\Pi$

$\rightarrow X^2\Sigma$), CH ($A^2\Delta \rightarrow X^2\Pi$), CO ($d^3\Delta \rightarrow a^3\Pi$), and C_2 ($A^3\Pi_g \rightarrow X^3\Pi_u$) also observed in CO_2 plasma afterglow region (33). The formation of these upper state ions and molecules in the air and CO_2 plasma region occurs due to the collision of gas (air or CO_2) with high-energy electrons, photons, ions, and neutral particles. These collisions result in the excited/upper vibration state of the above molecules. The most common reactions involved in these collisions were excitation, ionization, and dissociation (33-36). The details of air and CO_2 emission band peaks lines observed in the air and CO_2 plasma afterglow region are shown in Table S1 of supplementary material.

For air emission spectrum:



For CO_2 emission spectrum:



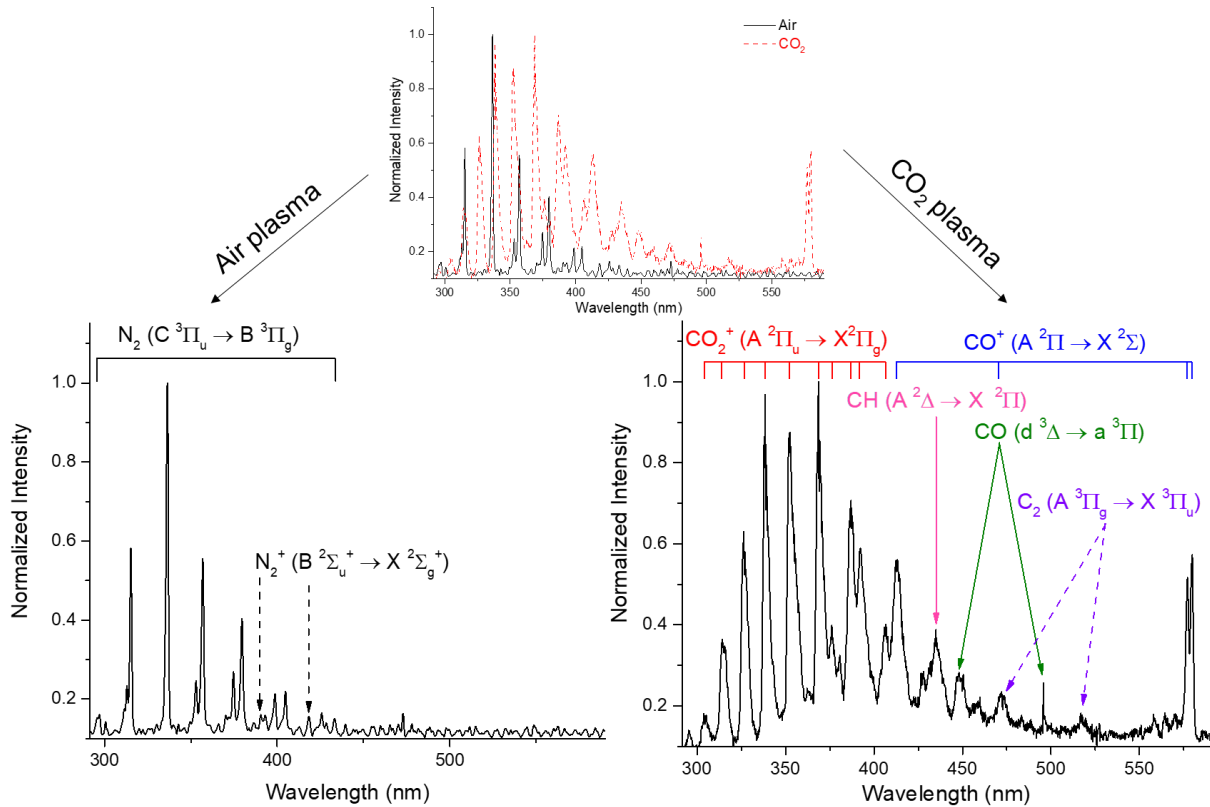


Figure 3. Air and CO₂ plasma emission spectra recorded in afterglow region

Physicochemical properties of plasma-activated water

The plasma-activated water (PAW) produced using air and CO₂ plasma is colorless in appearance. However, PAW (CO₂) and PAW (air) can be differentiated based on odor. PAW (air) was odorless, but PAW (CO₂) has a smoky and unpleasant odor.

The physicochemical properties of PAW produced using air and CO₂ plasma is shown in figure 4. The pH of PAW produced using air and CO₂ plasma showed a continuous decrease in its value with increasing plasma treatment time (figure 4 (a)). This signifies increasing

plasma-water treatment time results in more formation of acidic radicals/species in water (17, 22, 25). Moreover, the PAW produced using CO₂ plasma was considerably higher (82.14% higher after 60 minutes of treatment) than PAW produced using air plasma. Hence, the generated species in water when exposed to air plasma were more acidic compared to CO₂ plasma. Ma et al. (9) Subramanian et al. (1), El Shaer et al. (11), and Lu et al. (16) also showed a decrease in pH of PAW with increasing plasma treatment with water.

The oxidizing potential of PAW when produced using air and CO₂ plasma is shown in figure 4 (b). The oxidizing potential of PAW gives information regarding net combinations of oxidizing and reducing species formed in water after plasma exposure(12, 23, 25). The oxidation-reduction potential (ORP) of PAW prepared using air plasma was higher compared to PAW prepared using CO₂ plasma. This was due to the formation of a high concentration of oxidizing species in PAW when produced using air plasma compared to CO₂ plasma. For 60 minutes of plasma treatment, the ORP of PAW prepared using air plasma was 27.1% higher compared to CO₂ plasma. The increase in ORP of PAW with increasing plasma-water treatment is also shown in the work reported by Guo et al. (3), Xiang et al. (10), and Ma et al. (9), etc.

The rough estimation of conducting ions were measured by measuring total dissolved solids (TDS) and electrical conductivity (EC). The TDS and EC give the information regarding conducting ions formed in water due to plasma-water interaction. The observed TDS and EC of PAW, when prepared using air and CO₂ plasma are shown in figure 4 (c, d). Increasing plasma treatment with water increased the TDS and EC of PAW for both the air and CO₂ plasma. The observed TDS and EC of PAW prepared using air plasma were substantially high compared to CO₂ plasma (937.0% and 987.3% higher after 60 minutes of treatment). Hence, the concentration of inorganic ions formed in water after air plasma exposure was extremely higher compared to CO₂ plasma. The increase in EC with plasma treatment was also supported

by results of Subramanian et al. (1), Zhang et al. (37), and Sivachandiran et al. (15), and Lu et al. (16), etc.

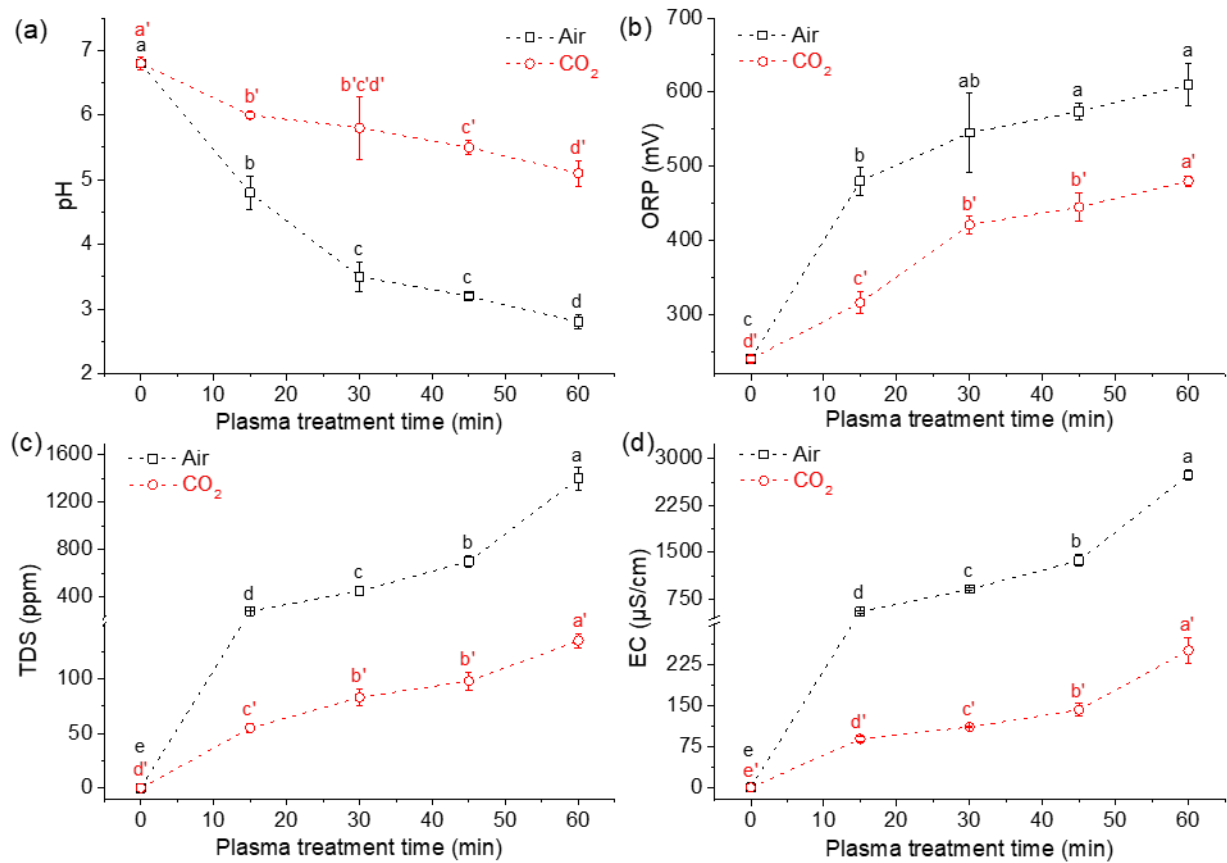
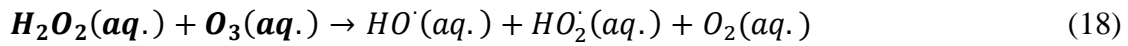
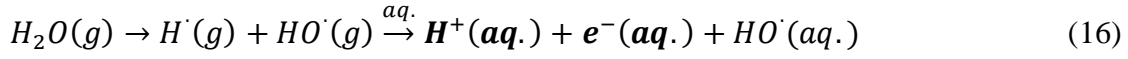


Figure 4. The variation in physicochemical properties of plasma activated water prepared using air and CO₂ plasma with plasma treatment time. (a) pH, (b) oxidation-reduction potential (ORP), (c) total dissolved solids (TDS), and (d) electrical conductivity (EC). Statistically significant ($p < 0.05$) difference between the group mean \pm standard deviation ($\mu \pm \sigma$) is shown by a different lowercase letter.

RONS concentration in plasma-activated water

The above-discussed variation in physicochemical properties of water after plasma treatment occurs due to the formation of numerous reactive species in water (1, 3, 4, 6-8, 14, 20, 22). The mechanism of formation of these reactive species in PAW is shown in equations (14-25) (1, 4, 12, 13, 16, 18, 22, 25).

Formation of reactive oxygen species (ROS) in plasma-activated water:



Formation of reactive nitrogen species (RNS) in plasma-activated water:

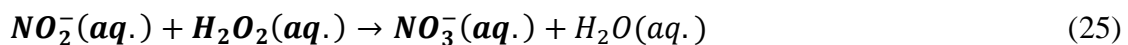
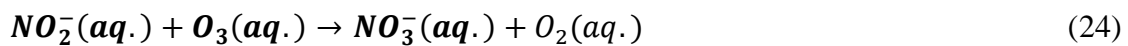
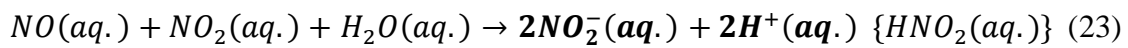
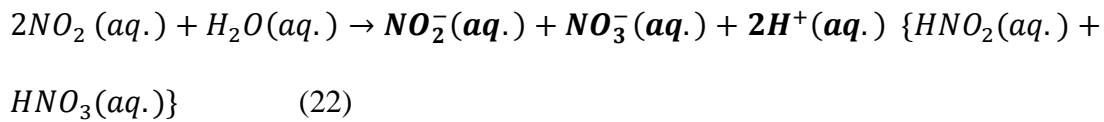
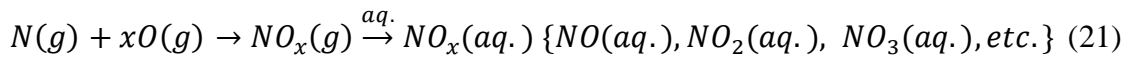


Figure 5 showed the identified and measured concentration of RONS (reactive oxygen-nitrogen species) present in PAW when prepared using air and CO₂ plasma. Figure 5 (a, c, e, g) showed the RONS such as NO₂⁻ ions, NO₃⁻ ions, H₂O₂, and dissolved O₃ in PAW when prepared using air plasma. The reactions involved in the formation of RONS in PAW (air) are given in equations (14-25 (16)). Moreover, the reactive species formed in PAW when using CO₂ plasma

are given as H_2O_2 , dissolved O_3 , dissolved CO_2 , and CO_3^{2-} ions (equations (14-19, 26-27)) (figure 5 (f, h) and figure 6).

The concentration of NO_3^- and NO_2^- ions present in PAW prepared using air and CO_2 plasma is shown in figure 5 (a-d). A continuous increase in NO_3^- and NO_2^- ions concentration with plasma treatment time observed in PAW prepared using air plasma (figure 5 (a, c)). The observed maximum concentration of NO_3^- and NO_2^- ions in PAW (air) were given as 4.0 mg L^{-1} and 401.5 mg L^{-1} , respectively. The NO_3^- and NO_2^- ions form nitric and nitrous acid in PAW (air) (equations (20-25)) (1, 6, 8, 12, 22). As nitric acid is a strong acid, therefore the lowest pH value of PAW (air) was given as 2.8. The increasing concentration of NO_2^- and NO_3^- ions with activation time was also reported by Subramanian et al. (1) and Xiang et al. (10) in PAW prepared in an air atmosphere. However, the PAW (CO_2) did not contain any observable concentration of NO_3^- and NO_2^- ions as shown in figure 5 (b, d). As discussed in equations (1-4, 20-23), the formation of RNS (reactive nitrogen species) in PAW required excited nitrogen species (12, 18, 22, 25) that were not observed in emission spectra of CO_2 plasma (figure 3). Hence, the possible RNS present in PAW (CO_2) such as (NO_2^- and NO_3^- ions) were beyond the detection limit of the present investigation.

Moreover, the concentration of H_2O_2 present in PAW (CO_2) was 316.7% higher than PAW (air). This was due to no interference of NO_2^- ions in H_2O_2 determination in PAW (CO_2). The NO_2^- ions present in PAW (air) react with H_2O_2 to give more stable NO_3^- ions (equation 25) (6, 18, 25). Therefore, interfere with the H_2O_2 determination in PAW (air). The interference of NO_2^- ions in H_2O_2 concentration and variation can be seen in figure 5 (e). Initially ($t = 0$ minutes), no H_2O_2 was present in PAW (air), as the plasma treatment increased to 30 minutes, a continuous increase in the H_2O_2 concentration was observed. Increasing plasma treatment time to 45 minutes results in a decrease in H_2O_2 concentration due to the reaction of NO_2^- ions with H_2O_2 to give more stable NO_3^- ions. Further increasing plasma treatment time to 60

minutes results in H_2O_2 concentration enhancement. This showed saturation of NO_2^- ions and H_2O_2 reaction in PAW (air) and the unreacted H_2O_2 shown by enhanced H_2O_2 in PAW (air). Similar behavior as H_2O_2 was observed in the concentration of dissolved O_3 in PAW (air). Since, NO_2^- ions present in PAW (air) also reacts with dissolved O_3 to give more stable NO_3^- ions by following equation (24). This rise and fall in H_2O_2 concentration in PAW (air) with increasing plasma treatment time also was observed in work reported by Subramanian et al. (1) and Sivachandiran et al. (15).

However, this rise and fall in H_2O_2 and dissolved O_3 concentration in PAW prepared using CO_2 plasma was not observed due to the absence of NO_2^- ions (figure 5 (b, d, g, h)). As no N_2 emission peaks bands were observed in the CO_2 plasma (figure 3) that confirms the absence of nitrogen species in CO_2 plasma. Hence, no interference of NO_2^- ions in PAW (CO_2) results in a monotonous increase in H_2O_2 and dissolved O_3 concentration with increasing plasma treatment time with water (figure 5 (g, h)).

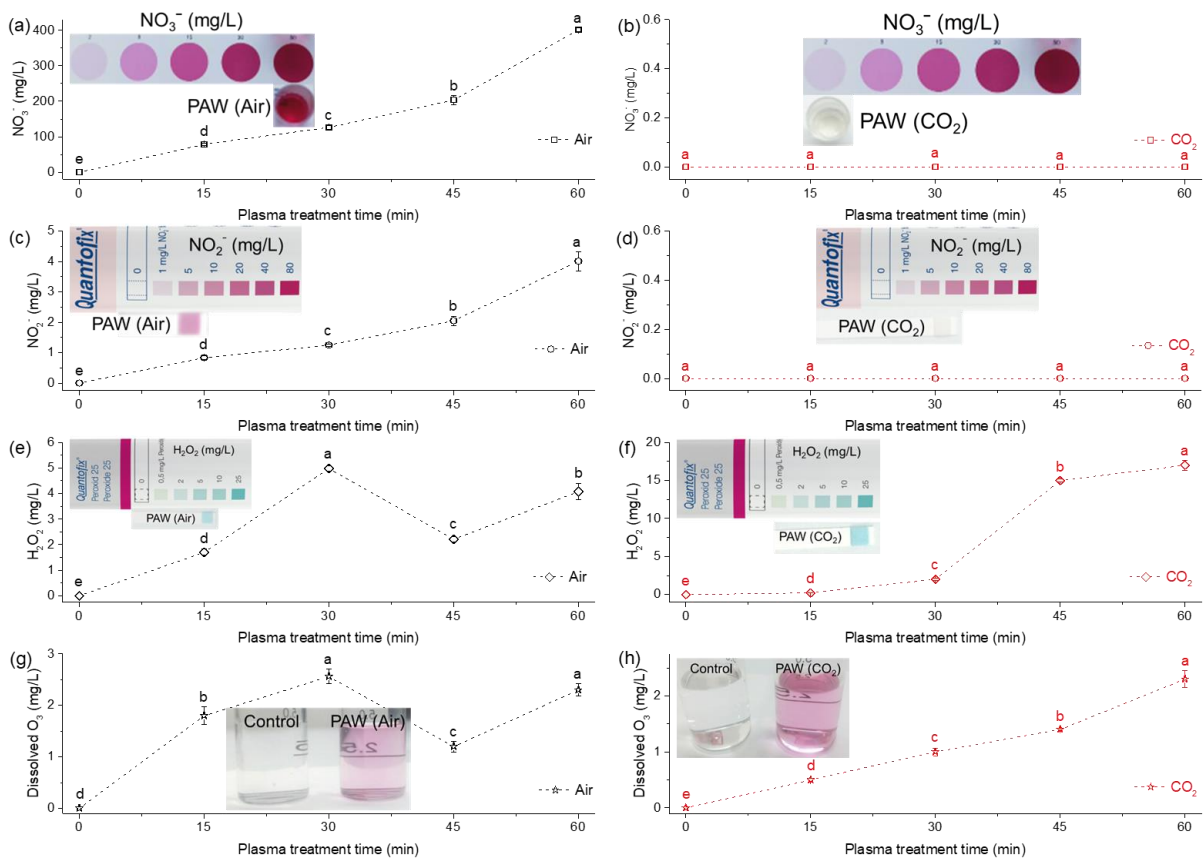


Figure 5. The variation in reactive oxygen-nitrogen species (RONS) concentration of plasma-activated water prepared using air and CO₂ plasma with plasma treatment time. (a, b) NO₃⁻ ions, (c, d) NO₂⁻ ions, (e, f) H₂O₂ concentration, and (g, h) Dissolved O₃. Statistically significant ($p < 0.05$) difference between the group mean \pm standard deviation ($\mu \pm \sigma$) is shown by a different lowercase letter.

The variation in titratable acidity, dissolved CO₂, and CO₃²⁻ ions with plasma treatment time in PAW (CO₂) is shown in figure 6. The excited carbon oxides (CO_x) and carbon oxide ions (CO_x⁺), etc. observed in emission spectra of CO₂ plasma (figure 3) when comes in contact with water enhances the solubility of CO₂ and formed carbonic acid (H₂CO₃), etc. in water (equations (26-27)(38)). Due to which physicochemical properties of PAW (CO₂) changed. The acidic species concentration formed in PAW (CO₂) was measured by measuring titratable acidity. Increasing plasma treatment time with water continuously and significantly ($p < 0.05$)

increases the titratable acidity, dissolved CO_2 , and CO_3^{2-} ions concentration. The uniform increase in titratable acidity, dissolved CO_2 , and CO_3^{2-} ions concentration signifies continuous production of reactive species in PAW (CO_2) with increasing plasma-water treatment time. The CO_3^{2-} ions exist in the form of carbonic acid in PAW (CO_2). The dissolved CO_2 and CO_3^{2-} ions (carbonic acid) are weak acids due to which the pH of PAW (CO_2) decreased. However, this decreases in pH of PAW (CO_2) significantly ($p < 0.05$) low compared to PAW (air).

Formation of carbonic acid in PAW:

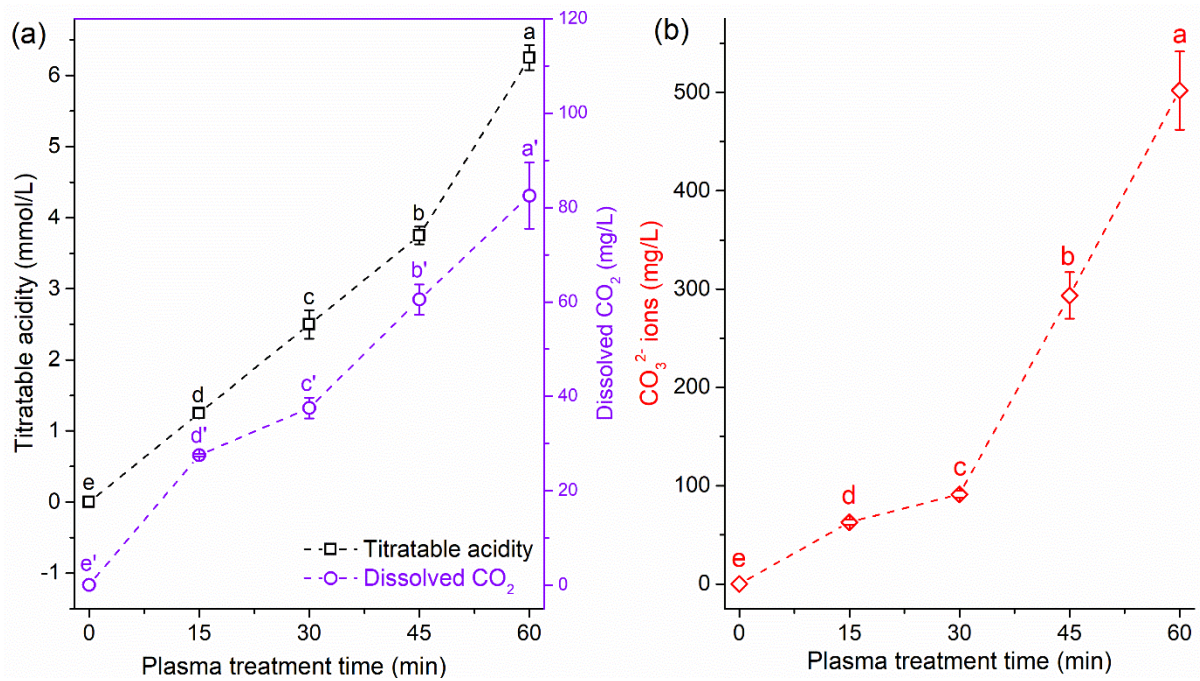
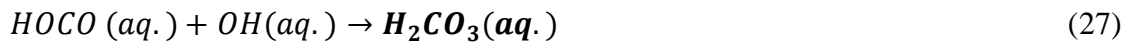


Figure 6. (a) Titratable acidity and dissolved CO_2 , and (b) CO_3^{2-} ions concentration in plasma-activated water produced using CO_2 plasma. Statistically significant ($p < 0.05$) difference between the group mean \pm standard deviation ($\mu \pm \sigma$) is shown by a different lowercase letter.

Hence, the above results and discussion showed the higher discharge current filaments in CO_2 plasma compared to air plasma. Moreover, the emission spectrum of CO_2 plasma is free from

nitrogen containing species. As a results, formation of reactive nitrogen species (RNS) is not occurring in PAW (CO₂). Hence, selective generation of reactive oxygen species (ROS) occurs in PAW (CO₂). Moreover, due to the use of CO₂ gas plasma for PAW preparation. The carbonic acid, dissolved CO₂, CO₃²⁻ ions also occurs in PAW due to which pH of PAW (CO₂) is decreased. However, the pH of PAW (CO₂) is significantly lower than PAW (air).

Conclusion

The present work compares the properties of PAW produced using air and CO₂ plasma. The acidity of PAW (air) is significantly higher than PAW (CO₂). This is due to the dissolution of strong acids (nitric acid) in PAW (air) compared to weak acids (carbonic acid) of PAW (CO₂). In addition, the oxidizing potential, total dissolved solids, and electrical conductivity of PAW (air) are significantly higher than PAW (CO₂). This is due to PAW (air) has high concentration of strong ionic species in the form of HNO₃ compared to weak H₂CO₃ species of PAW (CO₂). The PAW prepared using CO₂ plasma does not contain any reactive nitrogen species. This is due to the emission spectra of CO₂ plasma not containing any N₂ emission band peaks. Hence, CO₂ plasma-water interaction does not form any reactive nitrogen species in PAW (CO₂). Hence, selective production of reactive oxygen species can be achieved without the interference of reactive nitrogen species. Therefore, the concentration of dissolved H₂O₂ in PAW (CO₂) is higher than PAW (air). In conclusion, selective production of reactive oxygen species in plasma-activated water is possible by using CO₂ as a plasma-forming gas. The presence of reactive oxygen species in PAW (CO₂) makes it a useful antimicrobial agent. Moreover, it can also be used in numerous applications where conventional PAW could not be used due to its low pH (such as low pH PAW could not be used for surface disinfection of metal objects since it oxidizes its surface and damage it).

Acknowledgments

This work was supported by the Department of Atomic Energy (Government of India) doctrate fellowship scheme (DDFS).

Data availability statement

The data that support the findings of this study are available upon reasonable request from the authors.

Conflict of interests

The authors declare that there are no conflicts of interests.

Authors' contributions

Both authors contributed to the study conception and design. Material preparation, data collection, and analysis were performed by Vikas Rathore. The first draft of the manuscript was written by Vikas Rathore, and both authors commented on previous versions of the manuscript. Both authors read and approved the final manuscript.

ORCID iDs

Vikas Rathore <https://orcid.org/0000-0001-6480-5009>

References

1. Subramanian PG, Jain A, Shivapuji AM, Sundaresan NR, Dasappa S, Rao L. Plasma-activated water from a dielectric barrier discharge plasma source for the selective treatment of cancer cells. *Plasma Processes Polymers*. 2020;17(8):1900260.
2. Rathore V, Tiwari BS, Nema SKJPC, Processing P. Treatment of pea seeds with plasma activated water to enhance germination, plant growth, and plant composition. *Plasma Chemistry Plasma Processing*. 2022;42(1):109-29.

3. Guo J, Huang K, Wang X, Lyu C, Yang N, Li Y, et al. Inactivation of yeast on grapes by plasma-activated water and its effects on quality attributes. *Journal of food protection*. 2017;80(2):225-30.
4. Thirumdas R, Kothakota A, Annapure U, Siliveru K, Blundell R, Gatt R, et al. Plasma activated water (PAW): Chemistry, physico-chemical properties, applications in food and agriculture. *Trends in food science technology*. 2018;77:21-31.
5. Soni A, Choi J, Brightwell G. Plasma-activated water (PAW) as a disinfection technology for bacterial inactivation with a focus on fruit and vegetables. *Foods*. 2021;10(1):166.
6. Pan J, Li Y, Liu C, Tian Y, Yu S, Wang K, et al. Investigation of cold atmospheric plasma-activated water for the dental unit waterline system contamination and safety evaluation in vitro. *Plasma Chemistry Plasma Processing*. 2017;37(4):1091-103.
7. Sajib SA, Billah M, Mahmud S, Miah M, Hossain F, Omar FB, et al. Plasma activated water: The next generation eco-friendly stimulant for enhancing plant seed germination, vigor and increased enzyme activity, a study on black gram (*Vigna mungo* L.). *Plasma Chemistry Plasma Processing*. 2020;40(1):119-43.
8. Liu C, Chen C, Jiang A, Sun X, Guan Q, Hu W. Effects of plasma-activated water on microbial growth and storage quality of fresh-cut apple. *Innovative Food Science & Emerging Technologies*. 2020;59:102256.
9. Ma R, Wang G, Tian Y, Wang K, Zhang J, Fang J. Non-thermal plasma-activated water inactivation of food-borne pathogen on fresh produce. *Journal of hazardous materials*. 2015;300:643-51.
10. Xiang Q, Kang C, Niu L, Zhao D, Li K, Bai Y. Antibacterial activity and a membrane damage mechanism of plasma-activated water against *Pseudomonas deceptionensis* CM2. *LWT*. 2018;96:395-401.

11. El Shaer M, Eldaly M, Heikal G, Sharaf Y, Diab H, Mobasher M, et al. Antibiotics degradation and bacteria inactivation in water by cold atmospheric plasma discharges above and below water surface. *Plasma Chemistry Plasma Processing*. 2020;40(4):971-83.
12. Rathore V, Patil C, Sanghariyat A, Nema SK. Design and development of dielectric barrier discharge setup to form plasma-activated water and optimization of process parameters. *The European Physical Journal D*. 2022;76(5):1-14.
13. Lukes P, Dolezalova E, Sisrova I, Clupek MJPS, Technology. Aqueous-phase chemistry and bactericidal effects from an air discharge plasma in contact with water: evidence for the formation of peroxyxynitrite through a pseudo-second-order post-discharge reaction of H₂O₂ and HNO₂. *Plasma Sources Science Technology*. 2014;23(1):015019.
14. Rathore V, Desai V, Jamnapara NI, Nema SK. Activation of water in the downstream of low-pressure ammonia plasma discharge. *Plasma Research Express*. 2022;4(2):025008.
15. Sivachandiran L, Khacef A. Enhanced seed germination and plant growth by atmospheric pressure cold air plasma: combined effect of seed and water treatment. *RSC advances*. 2017;7(4):1822-32.
16. Lu P, Boehm D, Bourke P, Cullen PJ. Achieving reactive species specificity within plasma-activated water through selective generation using air spark and glow discharges. *Plasma Processes Polymers*. 2017;14(8):1600207.
17. Rathore V, Patel D, Shah N, Butani S, Pansuriya H, Nema SKJPC, et al. Inactivation of *Candida albicans* and lemon (*Citrus limon*) spoilage fungi using plasma activated water. *Plasma Chemistry Plasma Processing*. 2021;41(5):1397-414.
18. Rathore V, Patel D, Butani S, Nema SK. Investigation of physicochemical properties of plasma activated water and its bactericidal efficacy. *Plasma Chemistry Plasma Processing*. 2021;41(3):871-902.

19. Rashid M, Rashid M, Reza M, Talukder MJPC, Processing P. Combined Effects of Air Plasma Seed Treatment and Foliar Application of Plasma Activated Water on Enhanced Paddy Plant Growth and Yield. *Plasma Chemistry Plasma Processing*. 2021;41(4):1081-99.
20. Than HAQ, Pham TH, Nguyen DKV, Pham TH, Khacef AJPC, Processing P. Non-thermal plasma activated water for increasing germination and plant growth of *Lactuca sativa* L. *Plasma Chemistry Plasma Processing*. 2022;42(1):73-89.
21. Sukhani S, Punith N, Ekatpure A, Salunke G, Manjari M, Harsha R, et al. Plasma-Activated Water as Nitrogen Source for Algal Growth: A Microcosm Study. *IEEE Transactions on Plasma Science*. 2021;49(2):551-6.
22. Rathore V, Nema SK. A comparative study of dielectric barrier discharge plasma device and plasma jet to generate plasma activated water and post-discharge trapping of reactive species. *Physics of Plasmas*. 2022;29(3):033510.
23. Rathore V, Nema SKJPS. The role of different plasma forming gases on chemical species formed in plasma activated water (PAW) and their effect on its properties. *Physica Scripta*. 2022;97(6):065003.
24. Dryden M. Reactive oxygen species: a novel antimicrobial. *International journal of antimicrobial agents*. 2018;51(3):299-303.
25. Rathore V, Nema SK. Optimization of process parameters to generate plasma activated water and study of physicochemical properties of plasma activated solutions at optimum condition. *Journal of Applied Physics*. 2021;129(8):084901.
26. Fang Z, Xie X, Li J, Yang H, Qiu Y, Kuffel E. Comparison of surface modification of polypropylene film by filamentary DBD at atmospheric pressure and homogeneous DBD at medium pressure in air. *Journal of Physics D: Applied Physics*. 2009;42(8):085204.
27. Federation WE, Association A. Standard methods for the examination of water and wastewater: American Public Health Association: Washington, DC, USA; 2005.

28. Millero FJ, Zhang J-Z, Lee K, Campbell DM. Titration alkalinity of seawater. *Marine Chemistry*. 1993;44(2-4):153-65.
29. Saleem M, Choi NG, Lee KH. Facile synthesis of an optical sensor for CO_3^{2-} and HCO_3^- detection. *International Journal of Environmental Analytical Chemistry*. 2015;95(7):592-608.
30. Ghadami Jadval Ghadam A, Idrees M. Characterization of CaCO_3 nanoparticles synthesized by reverse microemulsion technique in different concentrations of surfactants. *Iranian Journal of Chemistry Chemical Engineering*. 2013;32(3):27-35.
31. Qayyum A, Zeb S, Ali S, Waheed A, Zakaullah MJPC, processing p. Optical emission spectroscopy of abnormal glow region in nitrogen plasma. *Plasma chemistry plasma processing*. 2005;25(5):551-64.
32. Shemansky D, Broadfoot A. Excitation of N_2 and $\text{N}^+ 2$ systems by electrons—I. Absolute transition probabilities. *Journal of Quantitative Spectroscopy Radiative Transfer*. 1971;11(10):1385-400.
33. Reyes P, Gómez A, Vergara J, Martínez H, Torres C. Plasma diagnostics of glow discharges in mixtures of CO_2 with noble gases. *Revista mexicana de física*. 2017;63(4):363-71.
34. Yoo S, Seok D, Jung Y, Lee K. Hydrophilic Surface Treatment of Carbon Powder Using CO_2 Plasma Activated Gas. *Coatings*. 2021;11(8):925.
35. Khan M, Rehman N, Khan S, Ullah N, Masood A, Ullah A. Spectroscopic study of CO_2 and $\text{CO}_2\text{-N}_2$ mixture plasma using dielectric barrier discharge. *AIP Advances*. 2019;9(8):085015.
36. Pearse RWB, Gaydon AG, Pearse RWB, Gaydon AG. The identification of molecular spectra: Chapman and Hall London; 1976.

37. Zhang Q, Ma R, Tian Y, Su B, Wang K, Yu S, et al. Sterilization efficiency of a novel electrochemical disinfectant against *Staphylococcus aureus*. *Environmental Science Technology*. 2016;50(6):3184-92.
38. Ioppolo S, Kaňuchová Z, James R, Dawes A, Ryabov A, Dezalay J, et al. Vacuum ultraviolet photoabsorption spectroscopy of space-related ices: formation and destruction of solid carbonic acid upon 1 keV electron irradiation. *Astronomy Astrophysics*. 2021;646:A172.